SUPPLEMENTAL DATA

Dysregulation of Glutathione Homeostasis Causes Oxido-reductive Stress and Cardiomyopathy in R120GCryAB Mice

Namakkal S. Rajasekaran, Patrice Connell, Elisabeth S. Christians, Liang-Jun Yan, Ryan P. Taylor, Andras Orosz, Xia Q. Zhang, Tamara J. Stevenson, Ronald M. Peshock, Jane A. Leopold, William H. Barry, Joseph Loscalzo, Shannon J. Odelberg, and Ivor J. Benjamin

EXPERIMENTAL PROCEDURES

Protein Isolation and Western Blot

Hearts were harvested from animals and flash frozen in liquid nitrogen. Tissue was pulverized and homogenized in 25mM HEPES, pH 7.4, 4 mM EDTA, 1.0 mM PMSF and Roche complete protease inhibitor cocktail. The extract was then centrifuged at 8,000-x g for 30 minutes at 4^{o}C. The pellet was then resuspended in 20mM Tris, pH 6.8, 1.0 mM EDTA and 1.0% SDS and briefly sonicated into solution. Protein concentrations for supernatant and pellet were determined using Bio-Rad protein assay kit. Equal amounts of protein extracts (10-20 μg) were loaded and separated by SDS-PAGE. Proteins were then transferred electrophoretically from the gels to Immobilon-P (Millipore) membrane. Blots were blocked in Tris Buffered Saline-Tween 20 (TBST) containing 5% (w/v) dry milk followed by incubation for 2 hrs with the respective primary antibody diluted in TBS buffer. Blots were then washed three times for 10 min each in TBST and incubated with anti-rabbit (1:25000) or anti-mouse (1:10000) IgG horseradish peroxidase (Vector Labs) conjugated secondary antibody in TBS for 1 hr. After washing 5 times for 10 min each in TBS, the membranes were treated with ECL detection reagents (Pierce, Amersham Bio) and the proteins were visualized by exposure to Blue sensitive biofilm (Hyblot Autoradiography, Denville Scientific, Inc.).

Immunoprecipitation and Immunoblotting

Heart homogenates were first prepared in TBS (10mM Tris, 150mM NaCl, pH 7.4) and centrifuged at 10,000 g for 15 minutes at 4 ^{0}C. The cytosol was used to immunoprecipitate CryAB, Hsp25 and G6PD proteins. About 100 µg of protein sample was incubated with the respective antibody and gently rotated for 12-14hrs, at 4 ^{0}C. 25 µl of protein-A sepharose beads were added to the antigen-antibody complex and continued the incubation for 3 hrs. The antigen-antibody-beads complex was then washed 5 times with IP buffer (HEPES -10mM, pH 7.4, NaCl – 50mM, glycerol – 10%, DTT – 1mM, and standard protease inhibitors). The final precipitate was diluted with 2X gel loading buffer and precipitated proteins were resolved in 10 or 12% PAGE and immunoblotted using respective antibodies. Similarly, reciprocal IP was performed to reveal the protein interactions.

Dissociation of Adult Mouse Ventricular Myocytes

Adult mouse myocyte isolation was performed with a modification of a previously described technique (Kadono et al., 2006). Briefly, hearts were removed from anesthetized mice and immediately attached to an aortic cannula. After perfusion with Ca^{2+}-free modified Tyrode's solution for 5 minutes, hearts were digested with 0.25 mg/mL liberase Blendzyme 1 (Roche Molecular Biochemicals) in 25 µmol/L $CaCl_2$–containing modified Tyrode's solution for 6-8 minutes. The solution consisted of (mmol/L) NaCl 126, KCl 4.4, $MgCl_2$ 1.0, $NaHCO_3$ 18, glucose 11, HEPES 4, and 0.13 U/mL insulin and was gassed with

5% CO_2/95% O_2, which maintained the pH at 7.4. The digested hearts were removed from the cannula, and the left ventricles were cut into small pieces in 100 µmol/L Ca^{2+} containing modified Tyrode's solution. These pieces were gently agitated and then incubated in the same solution containing 2% albumin at 30°C for 20 minutes. The cells were allowed to settle down with gravity. The supernatant was completely removed with a pipette and myocytes resuspended in 200 µmol/L Ca^{2+} and 2% albumin Tyrode's solution and allowed to settle for 20 minutes at 30°C. The cells were then resuspended in culture medium composed of 5% heat-inactivated fetal bovine serum (Hyclone), 47.5% MEM (GIBCO Laboratories), 47.5% modified Tyrode's solution, 10 mmol/L pyruvic acid, 4.0 mmol/L HEPES, and an additional 6.1 mmol/L glucose at 30°C in a 5% CO_2 atmosphere. The percentage of normal rod-shape myocytes was determined by phase contrast microscopy after 1 hour incubation in culture medium at 30°C in a 5% CO_2 atmosphere and was taken as an index of viability (Boston et al., 1998).

Isolated Heart Perfusion Studies

Mice were anesthetized with an intraperitoneal injection of 50 mg/Kg body weight of sodium pentobarbital. Hearts were weighed and myocardial function was evaluated at 37°C using an isolated Langendorff heart preparation as previously described (Neely et al., 1967). The modified Krebs perfusion buffer contained (in mM): 10 glucose, 1.75 $CaCl_2$, 118.5 NaCl, 4.7 KCl, 1.2 $MgSO_4$, 24.7 $NaHCO_3$, 0.5 EDTA, 12 mU/mL Insulin, and was gassed with 95% O_2-5% CO_2. Afterload was set by an 104 cm high aortic column (ID 3.18 mm), and

hearts were allowed to beat at their own intrinsic heart rate (HR) in a sealed water jacketed chamber maintained at 37°C. Hearts were initially perfused for 15 minutes with normal perfusate, then were switched to a perfusate solution containing 300 nM Dobutamine for 10 minutes to challenge the hearts as previously described (Arany et al., 2005), and finally returned to normal perfusate for the final 15 minutes of perfusion. An open-type catheter (20-gauge needle) was inserted into the left ventricle for determination of heart rate (HR) ventricular pressures (LVDP) and their derivatives (+/-dP/dt) with all data collected and analyzed at a sampling rate of 200 Hz using PowerLab (ADInstruments, Colorado Springs, CO). The data acquisition system was calibrated daily against a known column of perfusate at 0 mmHg and 80 mmHg. An open-type catheter was chosen over an isovolumetric intraventricular balloon because of the small and varying size of the mouse heart and evidence that this system determines changes in end-diastolic/developed pressure as accurately as a balloon insertion (Pahor et al., 1985; Sutherland et al., 2003). Coronary flow (CF), normalized for heart wet weight, was determined by timed collection and cardiac external work (RPP) is defined as the product of HR and LVDP. At the end of the perfusion period the beating hearts were frozen in liquid nitrogen and stored at -80°C for further analysis.

Noninvasive Measurements of Cardiac Function

Magnetic resonance imaging (MRI) was performed after animals were weighed and anesthetized with intraperitoneal injections of Avertin (2.5%

tribromoethanol and 0.8% 2-methyl-2-butanol in water, Sigma Chemicals) and monitored for normal respiratory function. The MRI scan was performed using a 1.5 T Philips Gyroscan NT whole body imaging system (Philips Medical Systems). The mouse was positioned supine in a 15 cm Petri dish and the electrocardiograph leads were attached to both front paws and one hindpaw. A standard finger coil was placed over the animal's chest and used for imaging the mouse heart. Heart rates were 380 to 450 beats per minute. Multislice, multiphase cine MRI was performed. Each study included a scout, coronal plane long axis of the left ventricle and a set of short axis acquisitions. Multiframe, short-axis gradient-echo sequences were used to measure LV end-systolic (LVESV) and diastolic volumes (LVEDV) as well as estimate LV mass and ejection fraction (EF). Four or five slices perpendicular to the long axis were obtained for each heart spanning from the apex to the base. The slice thickness was 1.6 mm with a 0.2 mm gap between slices. The pulse sequence was set for a heart rate of 210 bpm with nine cardiac phases and temporal resolution of 39ms. The frame with the largest chamber dimensions was used as end diastole for mass and volume measurements and the image with the smallest chamber volume was used for end systolic measures. The LV mass, LVEDV, LVESV and EF were determined from images and calculated as previously described (Franco et al., 1998; Franco et al., 1999). Initial groups (n=10-15/group) of experimental animals were assessed serially at 3, 6, and 10 months.

RNA Extraction and RNA Dot Blot Analyses

Anesthetized animals were perfused *in situ* with 10 ml of sterile PBS followed by 10 ml of RNAlater™ solution and hearts were immediately harvested. Atria were trimmed and the ventricles were immersed in RNAlater™ solution for 45 min at RT before frozen at –80^{o}C. Total RNA was extracted and purified from 25-30mg heart tissue using RNA Easy kit (QIAGEN,Valencia, CA), according to the manufacturer's instruction. RNA quality was monitored using Bio-analyzer and agarose gel electrophoresis. 1 μg of total RNA was diluted in Tris buffer, loaded and blotted on supercharged nylon membrane (BrighStar-plus, Ambion Inc.) using Biorad Biodot™ apparatus and the RNA was UV-cross linked to the membrane (Stratalinker, Stratagene). cDNA probes for atrial natriuretic factor (ANF), brain natriuretic factor (BNF), CryAB, and phospholamban (PLN) were generated using the following primer sets by PCR on mouse genomic DNA:

ANF (325 bp); left, 5' AACCTGCTAGACCACCTGGA-3';

right, 5'GGAAGCTGTTGCAGCCTAGT-3';

BNF (237 bp) left, 5' CACTGAAGTTGTTGTAGGAAGACC-3';

right, 5' CAAAAGCAGGAAATACGCTATG-3';

CryAB (300bp), left, 5' TCATCTCCAGGGAGTTCCAC-3';

right, 5' TAATCTGGGCCAGCCCTTAG-3';

and Phospholamban, left (PLN, 583 bp), left, 5' GCTGCCAATTTCCTCAACAT-3',

right, 5' ATCACAGCCAACACAGCAAG-3'.

PCR products from mouse genomic DNA were run on 1.5% agarose gel electrophoresis and fragments were purified using Qiaquick® gel extraction kit.

RNA blots were probed with respective α[^{32}P] dATP radiolabeled DNA probes, hybridized in Ultrahyb (Ambion) solution for 16-18 hours and washed according to the manufacturer's instruction. Membranes were then exposed to radiosensitive X-ray film (Hyblot CL Autoradiography, Denville Scientific Inc.) to detect hybridization signals using autoradiography for 16-24 hours. Levels of mRNA expression were obtained from scanned images and quantified using Image J analysis software.

Antioxidant Enzyme Activity Assays

Cytosolic activities of selected antioxidant enzymes were measured using commercially available kits from Bioxitech (OxisResearch). Catalase activity was determined using the Catalase-520TM assay in a two-step procedure (Aebi, 1984). Dismutation of hydrogen peroxide (H_2O_2) to water and molecular oxygen is proportional to the concentration of catalase. Diluted homogenates containing catalase were incubated in the presence of known concentration of H_2O_2. After incubation for 60 seconds, reaction was quenched with sodium azide. The amount of H_2O_2 remaining in the reaction mixture was then determined by the oxidative coupling reaction of 4-aminophenazone (4-aminoantipyrene, AAP) and 3,5-dichloro-2-hydroxybenzenesulfonic acid (DHBS) in the presence of H_2O_2 and catalyzed by horseradish peroxidase (HRP) and the resulting quinoneimine dye was measured at 520 nm.

The GPx-340™ assay is an indirect measure of the activity of cytosolic-GPx (Ursini et al., 1995). Oxidized glutathione (GSSG), produced in reduction of

organic peroxide by c-GPx, is recycled to its reduced state by the enzyme glutathione reductase (GSH-R). The oxidation of NADPH to $NADP^+$ is accompanied by a decrease in absorbance at 340 nm (A_{340}) providing a spectrophotometric means for monitoring GPx enzyme activity. To assay c-GPx, heart homogenate was added to a solution containing glutathione, glutathione reductase, and NADPH. The enzymatic reaction was initiated by adding the substrate, tert-butyl hydroperoxide, and the A_{340} was recorded. The rate of decrease in the A_{340} is directly proportional to the GPx activity in the sample. The GR-340 assay is based on the oxidation of NADPH to $NADP^+$ catalyzed by a limiting concentration of glutathione reductase (Beutler, 1969). One unit GSH-R activity in the homogenates is defined as the amount of enzyme catalyzing the reduction of one micromole of GSSG per minute at pH 7.6 and 25°C. The reduction of GSSG, determined indirectly by the measurement of the consumption of NADPH, decreases the absorbance at 340 nm (A_{340}) as a function of time.

Determination of Lipid Peroxides

Lipid peroxidation is a well-established mechanism of cellular injury and is used as an indicator of oxidative stress in cells and tissues *in vivo*. Lipid peroxides and modified products derived from polyunsaturated fatty acids are unstable and decompose to form complex compounds such as reactive carbonyl, the most abundant of which is malondialdehyde (MDA). The lipid peroxidation products, as MDA, were measured in the heart homogenates using the

thiobarbituric acid (TBA) reaction (Esterbauer and Cheeseman, 1990). In brief, 2.0 ml of 20% TCA supernatants from heart homogenates were mixed with 1.0% TBA reagent and boiled in a water bath for 15 minutes. The absorbance of the chromogen produced was measured at 532 nm in a Beckman UV-visible spectrophotometer.

Immunochemical Quantitation of Protein Carbonyls

Heart homogenates were prepared in 20mM Tris-HCl buffer, pH 6.8 containing 0.2% SDS and treated with 10mM Di-Nitro Phenyl Hydrazine (DNPH) as described previously (Yan and Sohal, 2000). The homogenates with DNPH were separated in 10% SDS-PAGE and probed against anti-DNPH antibody (Keller et al., 1993; Shacter et al., 1994). Nitrocellulose blots were incubated in 50 ml of 5% non-fat dried milk overnight at 4^{o}C and then washed with Tris-buffered saline (20mM Tris, 500mm NaCl pH 7.5), containing 0.1% Tween-20 (TBST), rinsed for 3 times (10 min each) and were incubated with primary rabbit anti-DNP antibody (1:2000 in TBST containing 0.2% BSA) for 2 hours at room temperature. Washes were repeated in TBST for 3 times before incubation with secondary rabbit IgG (diluted 1:25000 in TBST containing 0.2% BSA) for 1 hour at room temperature. After 5 washes (10 min each) in TBST, the blots were then treated with enhanced chemiluminescence (ECL, Amersham) detection kit. The signals for oxidized proteins were quantified using Image J densitometry software.

Results

MRI Studies of R120GCryAB Cardiomyopathy in Mice

We used magnetic imaging resonance (MRI) to assess the effects of hR120GCryAB expression on cardiac function *in vivo*. Serial measurements of ventricular cavity dimension, left ventricular mass (LVM) and left ventricular ejection fraction (LVEF) were made at 3, 6 and 10 months (Table S2). The hCryAB Tg mouse line, with mild wild-type CryAB overexpression, was selected as a control. At both 3 and 6 months, no differences in cavity dimension and cardiac function were observed in hCryAB Tg, hR120GCryAB Low Tg and hR120GCryAB High Tg animals (Table S2). There was a trend towards greater LV mass in hR120GCryAB Tg High mice compared with either hR120GCryAB Low Tg or hCryAB Tg at 6 months (Figure S1 and Table S2). Cardiac hypertrophy was most pronounced in hR120GCryAB High Tg mice at 10 months compared to hR120GCryAB Low Tg and/or hCryAB Tg (Table S2). Likewise, left ventricular ejection fraction was decreased at 10 months for hR120GCryAB High Tg compared with either hR120GCryAB Low Tg or hCryAB Tg animals (Table S2). These results indicate that cardiac hypertrophy and severe ventricular remodeling with dilatation are specific hallmarks of end-stage hR120GCryAB Tg protein aggregation cardiomyopathy in mice.

R120GCryAB Low Tg Mice Devoid of Large Aggregates Exhibit Decreased Cardiac Contractile Reserve

To assess the effects of hR120GCryAB Tg on cardiac myocyte viability, isolated left ventricular myocytes were cultured as described in Figure S2B (Boston et al., 1998). The survival of cardiomyocytes from age-matched, 6 month old hR120GCryAB High Tg was reduced by 30% compared with either hR120GCryAB Low Tg or NTg animals (Figure S2B). Both myocyte viability and cardiac function of hR120GCryAB Low Tg were normal between 12 and 40 weeks under basal conditions (Table S2), but mortality at 80 weeks was increased by 20 percent (Figure 1F). To determine if subtle cardiac abnormalities could be detected in hR120GCryAB Low Tg mice, we subjected experimental groups to 300 nM dobutamine challenge, an established method to assess cardiac reserve (Grupp et al., 1993). In the isolated perfused Langendorff heart, myocardial external work and maximal rates of contraction before, during, and after exposure to dobutamine revealed a myopathic effect of even mild hR120GCryAB overexpression compared to NTg (Figure S2C).

Biomarkers of Oxidative Stress Are Altered by hR120GCryAB Expression

Reactive oxygen species (ROS) have been implicated in the pathogenesis of cardiac hypertrophy and heart failure (Giordano, 2005; Griendling and FitzGerald, 2003; Yamamoto et al., 2003). We assessed the susceptibility of intracellular lipids and proteins to oxidative modifications as surrogate biomarkers. We measured lipid peroxidation using malondialdehyde (MDA) as a biomarker of oxidative stress (Figure S5A). We found that MDA was significantly and unexpectedly lower (by 40%) in hR120GCryAB High Tg hearts at 6 months

compared with the NTg control (Figure S5A). To corroborate these age-dependent effects, myocardial levels of protein carbonyl content were assessed by anti-dinitrophenylhydrazine (DNPH) immunostaining for specific amino acid residues modified by reactive oxygen species (Stadtman, 1992). At 3 and 6 months, tissue levels of anti-DNPH immunoreactive proteins were also elevated in both hCryAB Tg and hR120GCryAB Low Tg hearts compared with the NTg control (Figure S5B-C). In contrast, there was profound lowering of protein carbonyl levels in hR120GCryAB High Tg hearts between 3 and 6 months (Figure S5B-C). The unexpected lowering in the carbonyl content in hR120GCryAB High Tg hearts at 6 months is consistent with either an exaggerated increase in antioxidant enzymes (e.g., catalase, SOD) or marked enhancement in the reducing equivalents, or both.

References

Aebi, H. (1984). Catalase in vitro. Methods in Enzymology *105*, 121-126.

Arany, Z., He, H., Lin, J., Hoyer, K., Handschin, C., Toka, O., Ahmad, F., Matsui, T., Chin, S., Wu, P.H.*, et al.* (2005). Transcriptional coactivator PGC-1 alpha controls the energy state and contractile function of cardiac muscle. Cell Metabolism *1*, 259-271.

Beutler, E. (1969). Effect of flavin compounds on glutathione reductase activity: in vivo and in vitro studies. The Journal of Clinical Investigation *48*, 1957-1966.

Boston, D.R., Koyama, T., Rodriguez-Larrain, J., Zou, A., Su, Z., and Barry, W.H. (1998). Effects of angiotensin II on intracellular calcium and contracture in metabolically inhibited cardiomyocytes. J Pharmacol Exp Ther *285*, 716-723.

Esterbauer, H., and Cheeseman, K.H. (1990). Determination of aldehydic lipid peroxidation products: Malondialdehyde and 4-hydroxynonanol. Methods in Enzymology *186*, 407-420.

Franco, F., Dubois, S.K., Peshock, R.M., and Shohet, R.V. (1998). Magnetic resonance imaging accurately estimates LV mass in a transgenic mouse model of cardiac hypertrophy. Am J Physiol *274*, H679-683.

Franco, F., Thomas, G.D., Giroir, B., Bryant, D., Bullock, M.C., Chwialkowski, M.C., Victor, R.G., and Peshock, R.M. (1999). Magnetic resonance imaging and invasive evaluation of development of heart failure in transgenic mice with myocardial expression of tumor necrosis factor-alpha. Circulation *99*, 448-454.

Giordano, F.J. (2005). Oxygen, oxidative stress, hypoxia, and heart failure. J Clin Invest *115*, 500-508.

Griendling, K.K., and FitzGerald, G.A. (2003). Oxidative stress and cardiovascular injury: Part I: basic mechanisms and in vivo monitoring of ROS. Circulation *108*, 1912-1916.

Grupp, I.L., Subramaniam, A., Hewett, T.E., Robbins, J., and Grupp, G. (1993). Comparison of normal, hypodynamic, and hyperdynamic mouse hearts using isolated work-performing heart preparations. Am J Physiol *265*, H1401-1410.

Kadono, T., Zhang, X.Q., Srinivasan, S., Ishida, H., Barry, W.H., and Benjamin, I.J. (2006). CRYAB and HSPB2 deficiency increases myocyte mitochondrial permeability transition and mitochondrial calcium uptake. J Mol Cell Cardiol *40*, 783-789.

Keller, R.J., Halmes, N.C., Hinson, J.A., and Pumford, N.R. (1993). Immunochemical detection of oxidized proteins. Chem Res Toxicol *6*, 430-433.

Neely, J.R., Liebermeister, H., Battersby, E.J., and Morgan, H.E. (1967). Effect of pressure development on oxygen consumption by isolated rat heart. Am J Physiol *212*, 804-814.

Pahor, M., Di Gennaro, M., Cocchi, A., Bernabei, R., Carosella, L., and Carbonin, P. (1985). Age-related incidence of reperfusion- and reoxygenation-induced ventricular tachyarrhythmias in the isolated rat heart. Gerontology *31*, 15-26.

Shacter, E., Williams, J.A., Lim, M., and Levine, R.L. (1994). Differential susceptibility of plasma proteins to oxidative modification: examination by western blot immunoassay. Free Radic Biol Med *17*, 429-437.

Stadtman, E.R. (1992). Protein oxidation and aging. Science *257*, 1220-1224.

Sutherland, F.J., Baker, K.E., Shattock, M.J., and Hearse, D.J. (2003). Responses to ischaemia and reperfusion in the mouse isolated perfused heart and the phenomenon of 'contractile cycling'. Clinical and Experimental Pharmacology & Physiology *30*, 879-884.

Ursini, F., Maiorino, M., Brigelius-Flohe, R., Aumann, K.D., Roveri, A., Schomburg, D., and Flohe, L. (1995). Diversity of glutathione peroxidases. Methods in Enzymology *252*, 38-53.

Yamamoto, M., Yang, G., Hong, C., Liu, J., Holle, E., Yu, X., Wagner, T., Vatner, S.F., and Sadoshima, J. (2003). Inhibition of endogenous thioredoxin in the heart increases oxidative stress and cardiac hypertrophy. J Clin Invest *112*, 1395-1406.

Yan, L.J., and Sohal, R.S. (2000). Analysis of oxidative modification of proteins. In Current Protocols in Protein Sciences, J.E. Coligan, B.M. Dunn, H.L. Ploegh, D.W. Speicher, and P.T. Wingfield, eds. (New York, John Wiley & Sons, Inc.), pp. 14.14.11-14.14.24.

FIGURE LEGENDS

Figure S1. Cross-sections from magnetic resonance imaging performed on transgenic hCryAB Tg (A), hR120GCryAB Low Tg, and hR120GCryAB High Tg mice at 6 months.

Figure S2. Immunohistofluorescence, cellular viability of isolated cardiomyocytes, and cardiac contractile reserve of hR120GCryAB Low Tg animals.

(A) Nontransgenic (NTg) heart exhibits very little fluorescent staining (green) against anti-human αB-crystallin (hCryAB). Confocal images of myocardial section were counterstained with phalloidin (red fluorescence). No aggregates are seen in myocardial sections of hR120GCryAB Low Tg animals.

(B) Viability of left ventricular myocytes from hR120GCryAB High Tg is decreased 1 hour after isolation compared with either hR120GCryAB Low Tg or NTg controls (Mean±SEM, n=4 isolations for each group). *$p < 0.05$

(C) Mild level of human R120GCryAB overexpression significantly reduces external work (rate pressure product, RPP) calculated as the product of heart rate (HR) and left ventricular developed pressure (LVDP) compared with NTg controls at 6 months. Drug infusion (300 nM Dobutamine) was started at 15 minutes and terminated at 25 minutes in the isolated perfused Langendorff heart. Experimental groups contain 6 animals/group. Values are mean ± SE. NTg, non-transgenic control; hR120GCryAB Low Tg. *($p<0.05$) NTg vs. hR120GCryAB Low Tg.

Figure S3. Hypertrophic markers in R20GCryAB cardiomyopathy at 6 months.

Several molecular markers of the hypertrophic response such as atrial natriuretic factor (ANF) and brain natriuretic factor (BNF) were significantly increased in hR120GCryAB High Tg animals while phospholamban (PLN) was decreased compared with controls. In these RNA blots, each spot represents an individual animal per experimental group (3 animals/group). (*$p < 0.05$ for all panels).

Figure S4. Protein expression of Hsp25 at 2 month.

The myocardial levels of Hsp25 protein were not significantly different in either supernatant or pellet among 2 month old NTg, hCryAB Tg, hR120GCryAB Low Tg and hR120GCryAB High Tg mice.

Figure S5. Markers of oxidative stress are altered by R120GCryAB expression.

(A) Human R120GCryAB overexpression paradoxically decreases levels of lipid peroxidation assessed as TBA-reacting malondialdehyde (MDA) in hR120GCryAB High Tg at 6 months (NTg vs. hR120GCryAB High Tg; 1.03±0.16 and 0.59±0.13, $p<0.05$).

(B) Protein carbonylation was decreased in hR120GCryAB High Tg hearts compared with either NTg or hR120GCryAB Low Tg hearts at 6 months. Immunoblots of protein carbonylation, a biomarker for redox stress, were

obtained from TCA supernatants of the DNPH-treated heart homogenates, which were separated by SDS-PAGE and then probed with rabbit anti-DNP antibody.
(C) Densitometry analysis of the DNPH blot shows a 50% reduction of carbonylated proteins in the 6 month old hR120GCryAB High Tg hearts, consistent with increased reductive stress in these mice.
(D) The corresponding representative gel (panel B) after Coomassie staining is shown.

Figure S6. G6PD deficiency reverses several biomarkers of cardiac hypertrophy in hR120GCryAB High Tg/G6PD^{mut} *in vivo*.

G6PD deficiency attenuated several molecular markers of the hypertrophic response such as brain natriuretic factor (BNF) and phospholamban (PLN) in hR120GCryAB High Tg expression crossed into G6PD^{mut} animals. Messenger RNA level of sarcoplasmic-endoplasmic reticulum Ca^{2+} ATPase 2A (SERCA 2A) was increased in hR120GCryAB High Tg compared with NTg and was not significantly different between hR120GCryAB High Tg and the hR120GCryAB High Tg/G6PD^{mut} intercross. Each spot represents an individual animal per experimental group (3 animals/group). (* signifies $p<0.05$ for all panels).

Table S1

Heart, body and heart / body weight ratio for NTg, hCryAB Tg, hR120GCryAB Low Tg, hR120GCryAB High Tg mice at 3 and 6 months of age.

Groups	3 months			6 months		
	Heart wt (mg)	Body wt (g)	HW/BW	Heart wt (mg)	Body wt (g)	HW/BW
Non transgenic	119.65 ± 9.65	25.67 ± 1.78	4.69 ± 0.44	131.03 ± 15.75	29.01 ± 3.35	4.60 ± 0.35
hCryAB Tg	119.75 ± 8.83	25.57 ± 1.87	4.73 ± 0.27	140.05 ± 15.46	32.12 ± 3.25	4.36 ± 0.48
hR120GCryAB Low Tg	112.83 ± 13	26.6 ± 4.4	4.42 ± 0.3	128.28 ± 11.97	27.98 ± 2.79	4.61 ± 0.38
hR120GCryAB High Tg	126.75 ± 8.90	25.91 ± 2.21	5.03 ± 0.32	165.21 ± 11.70*	27.68 ± 2.09	6.07 ± 0.56*

Data represent the mean ± SD for > 15 animals. * Heart weight and HW/BW ratio are significantly different in hR120GCryAB High Tg when compared to NTg or other groups at 6 months, $p<0.01$. HW = Heart weight; BW = Body weight; hCryAB Tg = Wild-type CryAB transgenic lines; Transgenic lines that express mild and moderate amounts of hR120G CryAB are designated hR120GCryAB Low Tg and hR120GCryAB High Tg, respectively.

TABLE S2

Magnetic Resonance Imaging data

Transgene Expressed	Age			*p* value intragroup
	3 months	6 months	10 months	
hCryAB Tg				
BW, g	28.3 ± 2.02	30.6 ± 1.56	35.5 ± 2.28	ND
LV mass, mg	82.7 ± 2.82	93.2 ± 2.17	94.7 ± 3.36	< 0.02
LV EDV, µl	40.8 ± 2.89	39.4 ± 1.86	49.7 ± 2.17	Not significant
LV ESV, µl	16.1 ± 1.27	12 ± 2.15	19.2 ± 1.47	Not significant
LV EF	57.5 ± 3.24	67.8 ± 4.99	61.3 ± 3.75	Not significant
n	12	12	11	
hR120GCryAB Low Tg				
BW, g	24.4 ± 0.96	25.8 ± 2.55	35 ± 2.09	ND
LV mass, mg	78.3 ± 2.79	88.1 ± 2.81	101.6 ± 5.45	< 0.002
LV EDV, µl	41.5 ± 2.01	45.3 ± 2.17	55.1 ± 3.73	< 0.005
LV ESV, µl	15.3 ± 1.49	18.4 ± 2.21	23.7 ± 1.98	< 0.005
LV EF	64.6 ± 3.27	59.8 ± 4.24	57 ± 3.26	Not significant
n	16	12	7	
hR120GCryAB High Tg				
BW, g	24.4 ± 1.15	26.3 ± 0.92	35.2 ± 2.87	ND

LV mass, mg	88.3 ± 3.98	103.6 ± 4.77	129.8 ± 6.93[a]	0.0001
LV EDV, µl	41.8 ± 1.59	47.4 ± 2.93	61 ± 4.46	< 0.0005
LV ESV, µl	14.6 ± 1.26	21 ± 2.3993[b]	36.4 ± 7.46[c]	< 0.0005
LV EF	65.5 ± 2.19	54.2 ± 4.46	41.3 ± 9.2346[d]	< 0.02
n	12	8	5	

LV = left ventricle; EDV = end-diastolic volume; ESV = end-systolic volume; EF = ejection fraction; ND = not determined; BW = Body weight. hCryAB Tg = Wild-type CryAB transgenic line; Transgenic lines that express mild and moderate amounts of hR120GCryAB are designated hR120GCryAB Low Tg and hR120GCryAB High Tg, respectively.

[a] indicates a significant difference when hCryAB Tg is compared to other groups with a *p* value=0.0002.

[b] indicates a significant difference when hCryAB Tg is compared to other groups with a *p* value=0.005 at 6 months.

[c] indicates a significant difference when hCryAB Tg is compared to other groups with a *p* value=0.01 at 10 months.

[d] indicates a significant difference when hCryAB Tg is compared to other groups with a *p* value=0.02 at 10 months.

FIGURE S1


A
hCryAB Tg
B
hR120GCryAB Low Tg
C
hR120GCryAB High Tg
6 months
Chest wall
Right Ventricular Cavity
Interventricular Septum
Left Ventricular Cavity

FIGURE S2

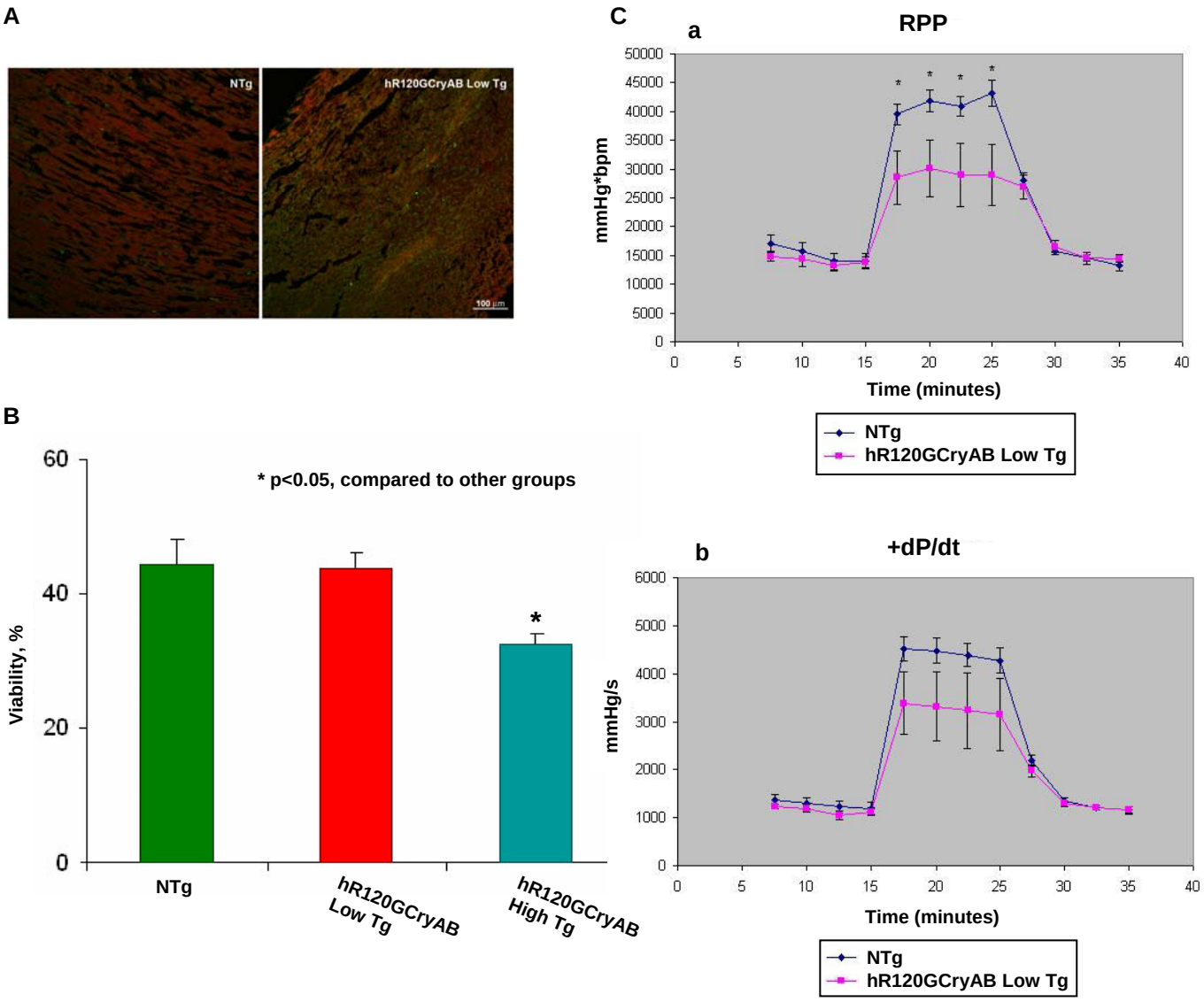
A
NTg
hR120GCryAB Low Tg
100 µm
B
* p<0.05, compared to other groups
Viability, %
60
40
20
0
*
NTg
hR120GCryAB Low Tg
hR120GCryAB High Tg
C
a
RPP
mmHg*bpm
50000
45000
40000
35000
30000
25000
20000
15000
10000
5000
0
0 5 10 15 20 25 30 35 40
Time (minutes)
NTg
hR120GCryAB Low Tg
b
+dP/dt
mmHg/s
6000
5000
4000
3000
2000
1000
0
0 5 10 15 20 25 30 35 40
Time (minutes)
NTg
hR120GCryAB Low Tg

FIGURE S3

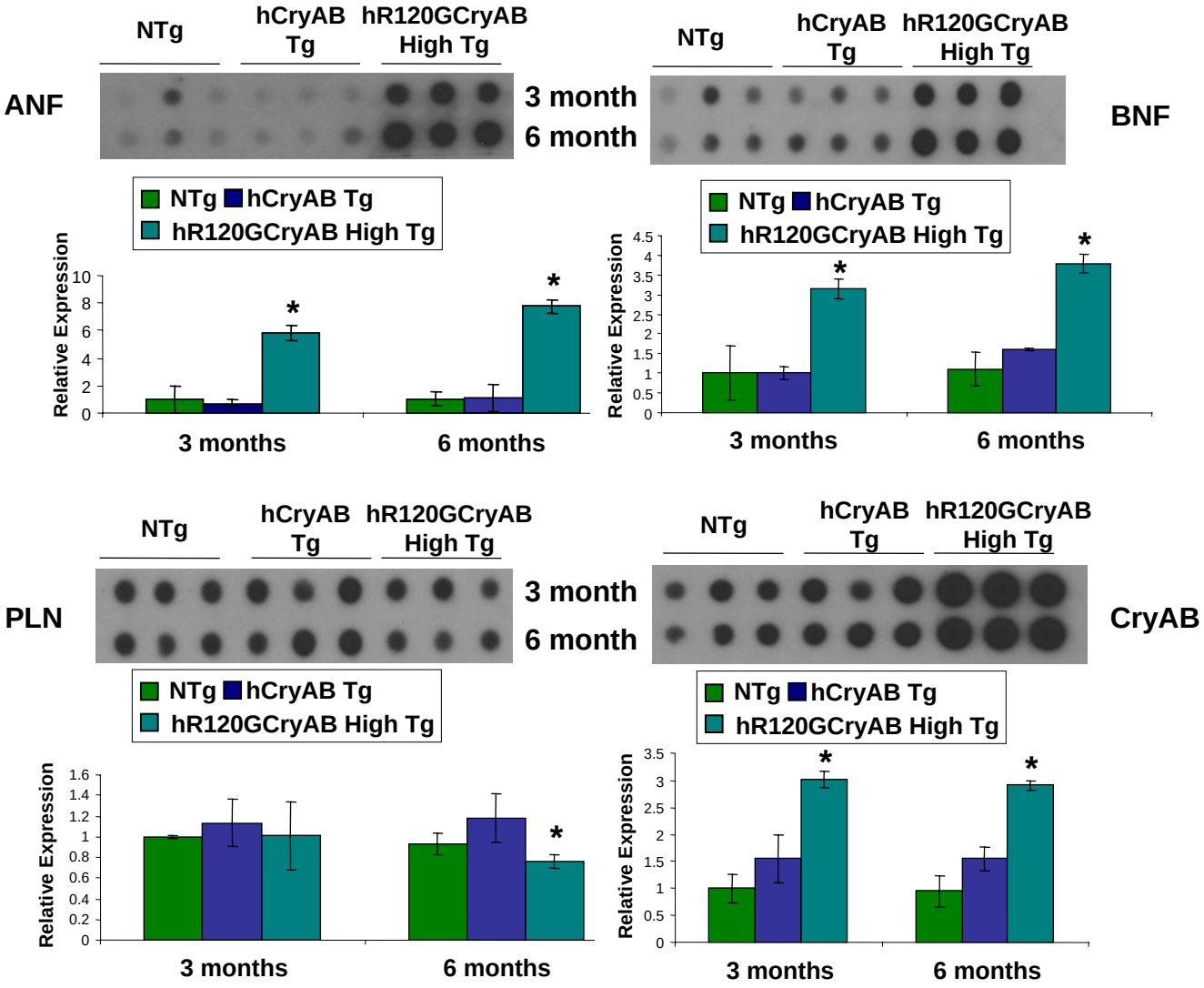
NTg
hCryAB Tg
hR120GCryAB High Tg
ANF
3 month
6 month
BNF
NTg hCryAB Tg
hR120GCryAB High Tg
Relative Expression
3 months
6 months
PLN
CryAB

FIGURE S4

A Hsp25 PROTEIN EXPRESSION FOR MICE AT 2 MONTHS

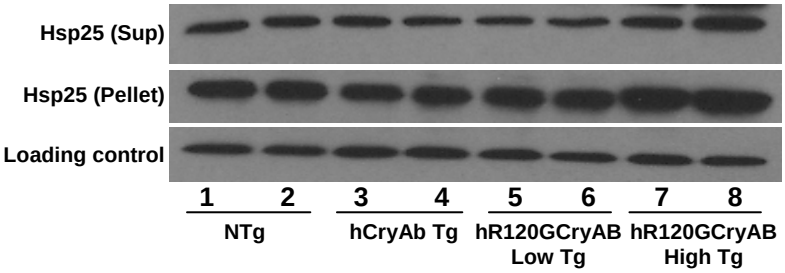

B

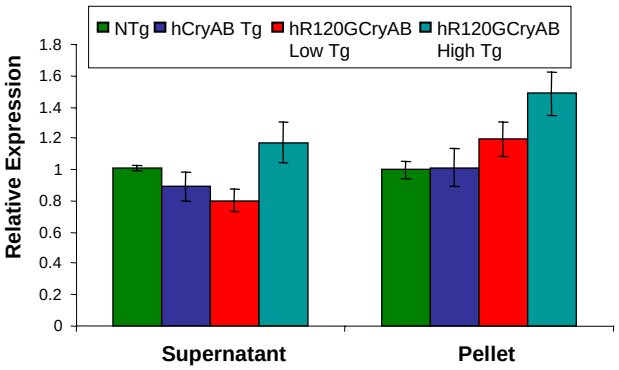

FIGURE S5

A LIPID PEROXIDATION ASSAY

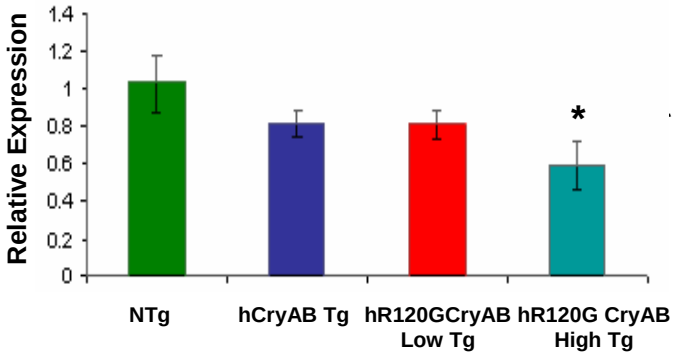

B ANTI-DNPH WESTERN BLOT FOR CARBONYLATED PROTEINS

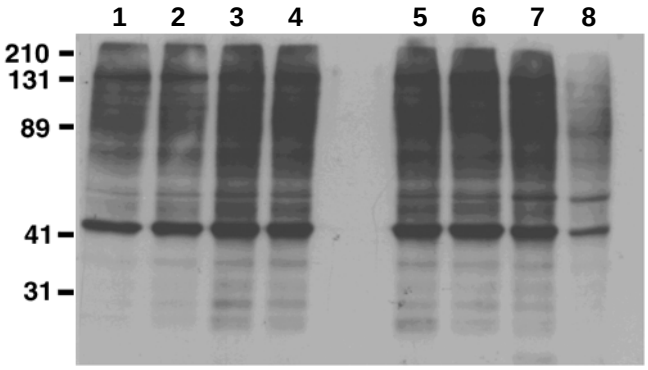

1- NTg – 3 months
2- NTg – 6 months
3- hCryAB Tg – 3 months
4- hCryAB Tg – 6 months
5- hR120GCryAB Low Tg – 3 months
6- hR120GCryAB Low Tg – 6 months
7- hR120GCryAB HighTg – 3 months
8- hR120GCryAB High Tg – 6 months

C DENSITOMETRY

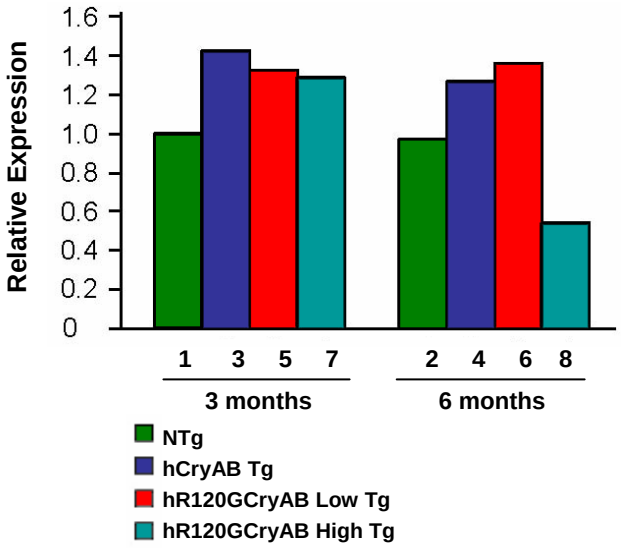

D COOMASSIE-STAINED GEL FOR LOADING COMPARISON

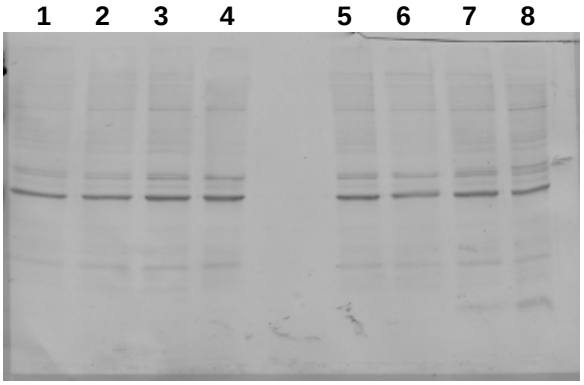

1- NTg – 3 months
2- NTg – 6 months
3- hCryAB Tg – 3 months
4- hCryAB Tg – 6 months
5- hR120GCryAB Low Tg – 3 months
6- hR120GCryAB Low Tg – 6 months
7- hR120GCryAB High Tg – 3 months
8- hR120GCryAB High Tg – 6 months

FIGURE S6

RNA DOT BLOTS